(Received 19 December 2023, Accepted 5 January 2024, Scheduled 18 January 2024)

A High Performance Duplexer Based on Dual-Mode E-Type Resonator

Mingxin Liu[1, 2, 3, *], Mingfu Li[1, 2], Hui Li[2], and Yan Chen[1]

[1] *Postdoctoral Innovation Practice Base, Chengdu Textile College, Chengdu 611731, China*
[2] *School of Aeronautics and Astronautics, University of Electronic Science and Technology of China, Chengdu 611731, China*
[3] *School of Unmanned Aerial Vehicles Industry, Chengdu Aeronautic Polytechnic, Chengdu 610100, China*

ABSTRACT: A novel compact planar duplexer is proposed. It consists of three dual-mode E-shaped microstrip resonators and works well on the WCDMA system with uplink band of 1940 MHz–1955 MHz and downlink band of 2130 MHz–2145 MHz. The high rectangular coefficient of the duplexer makes its frequency selectivity high, and its small size is convenient for further miniaturization. In the product test, the duplexer is found to meet the band requirements very well with high isolation levels of −44 dB and −48 dB at the first and second frequency centers, respectively, which are better than those with similar frequency bands in the references.

1. INTRODUCTION

In wireless communication system, the duplexer is one of the key components in selecting channels, synthesizing signals, and separating frequencies. In recent years, it has been increasingly used in modern high-speed wireless systems such as GSM, CDMA, and UMTS-WCDMA [1–7].

The most commonly used duplexer is to combine two bandpass filters into a three-port impedance matching network [8–10]. A large-sized T-shaped joint circuit is widely adopted in the combination to produce good transmission in one passband and good attenuation in the other. To reduce the large size of the T-shaped joint circuit, compact designs are proposed [11, 12]. Another good way to largely reduce the size is to minimize the two filters by designing a public resonator within the circuit instead of the T-shaped circuit [13, 14]. The public resonator makes a transmission pole in each passband, thus it is able to reduce the total number of resonators needed by the duplexer. However, it remains tough to design compact high-isolation duplexers by using dual-mode resonators.

This paper proposes the novel design of a compact high-isolation duplexer by using dual-mode resonators. It consists of three dual-mode E-shaped microstrip resonators, where two resonant-mode resonators are coupled to the third single-mode stub-loaded resonator, so its frequency band covers both the uplink frequency passband of 1940 MHz–1955 MHz and downlink frequency passband of 2130 MHz–2145 MHz of the WCDMA system. Firstly, two bandpass filters in accordance with the WCDMA frequency bands are designed based on the structures of the two microstrip E-shaped resonators. Then in the input section of the duplexer, an E-shaped public resonator is developed. Finally, by product measurements, the duplexer is found to meet the frequency band requirements very well, with the isolation levels of the two passbands reaching as high as 40 dB and 35 dB. When being installed on antennas with transmitter-receiver isolated system, the duplexer can ensure a proper running by its good separation of the transmitted and received signals.

* Corresponding author: Mingxin Liu (lmx0951@163.com).

2. ANALYSIS OF THE DUAL-MODE E-SHAPED RESONATORS

The structure and sizes of the proposed duplexer are shown in Figure 1 and Table 1, which consists of three dual-mode stub-loaded resonators, where the input port 1 is of an E-shaped fold structure, and port 2 and port 3 are both E-shaped bandpass filters. An interdigitated capacitor structure is adopted in port 1 for the power feed of the duplexer, increasing the bandwidth and coupling magnitude at the same time. The dielectric substrate used in the proposed design is Rogers 4003 with a thickness of 0.508 mm, a relative dielectric coefficient of 3.55, and a dielectric loss angle tangent of 0.0027.

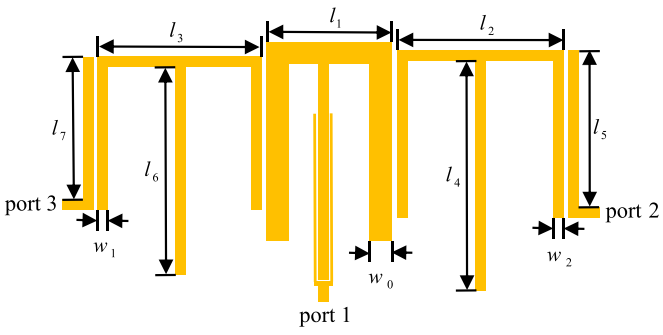

FIGURE 1. Structure and sizes of the proposed duplexer.

Figure 2(a) shows the entire structure of the E-shaped dual-mode resonator, along with the length L_1 and characteristic admittance Y_1 of the two side branches and the length L_2 and characteristic admittance Y_2 of the central branch, where the symmetric structure of the resonator allows its resonance char-

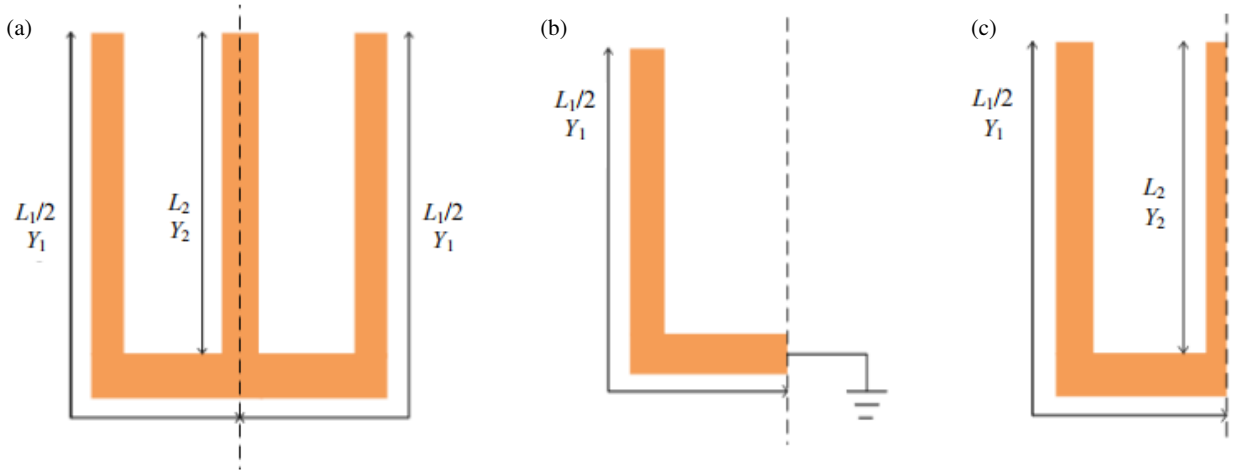

FIGURE 2. (a) Overall structure of the E-shaped dual-mode resonator; (b) Equivalent circuit in the odd-mode; (c) Equivalent circuit in the even-mode.

TABLE 1. Numeric values of sizes.

Parameter	Numeric Value	Parameter	Numeric Value
l_1	12 mm	l_2	16 mm
l_3	15.8 mm	l_4	23 mm
l_5	15.1 mm	l_6	21 mm
l_7	13.7 mm	w_0	2 mm
w_1	1 mm	w_2	1 mm

acteristics to be analyzed by the odd-mode and even-mode. The dotted line shown in Figure 2(a) can be equated to an electric wall in the odd-mode and a magnetic wall in the even-mode. Figure 2(b) shows its corresponding electric wall in odd-mode of a ground fault. Figure 2(c) shows its corresponding magnetic wall of an open circuit in even-mode.

The input admittance of the grounding microstrip in the odd-mode is

$$Y_{ino} = \frac{Y_1}{j\tan(\theta_1/2)} \tag{1}$$

where $\theta_1 = \beta L_1$ is the length of the sided branch microstrip, and β is the phase parameter in electromagnetic wave propagation. The input admittance of the open microstrip in the even-mode is

$$Y_{ine} = jY_1 \frac{2Y_1\tan(\theta_1/2) + Y_2\tan(\theta_2)}{2Y_1 - Y_2\tan(\theta_1/2)\tan(\theta_2)} \tag{2}$$

where $\theta_2 = \beta L_2$ is the length of the central branch microstrip. The resonant frequencies in the odd-mode and even-mode can be obtained from $Y_{ino} = Y_{ine} = 0$:

$$f_{odd} = \frac{(2n-1)c}{2L_1\sqrt{\varepsilon_{eff}}} \tag{3}$$

$$f_{even} = \frac{nc}{(2L_2 + L_1)\sqrt{\varepsilon_{eff}}} \tag{4}$$

where $n = 1, 2, 3\cdots$, c is the light speed in a vacuum, and ε_{eff} is the effective dielectric constant of the microstrip. In the even-mode, f_{even} varies with the length of the central branch microstrip. By letting L_2 approach the wavelength of the guided waves with a quarter of the resonant frequency, and by setting the resonant frequencies of the other two loaded resonators close to f_{even}, we can make the characteristics of a filter circuit appear.

3. ANALYSIS OF THE TRANSMISSION POLES AND ZEROS

Transmission zero appears when the length of the central branch L_2 approaches the wavelength of the guided waves with a quarter of the resonant frequency. The location of the zero can be adjusted by changing the value of L_2. For power feed resonators, the location of the transmission zero should be placed between the two pass bands at some frequency. One transmission zero is designed to be in the upper stopband of the lower frequency bandpass filter and the other in the lower stopband of the higher frequency bandpass filter. In this way, the lower passband and higher passband are well separated to minimize their mutual interference. The followings are the detailed analysis of the transmission zeros.

It is found that a symmetric E-shaped resonator itself can produce outside the passband a transmission zero that depends on f_{odd} and f_{even}. The zero point appears to the left of the passband if $f_{even} < f_{odd}$, and to the right if $f_{odd} < f_{even}$. The half-wavelength central branch microstrip of the E-shaped resonator shown in Figure 2(a) is with one end open. The open microstrip is equivalent to an LC circuit in a lumped circuit. It is the same as a capacitor or inductor in the case of no loss when there is no resonation. If resonation occurs, the equivalent impedance of the open microstrip becomes zero, thus it is like a short component connected in parallel with the center of the microstrip, so there will be no signal transmission, and thus a zero point appears at the resonant frequency, which explains how the transmission zero comes into being.

Figure 3 illustrates the coupling of the proposed duplexer. The two modes M_1 and M_1' of the central public E-shaped DMR_1 (Dual Mode Resonator 1) produce two different res-

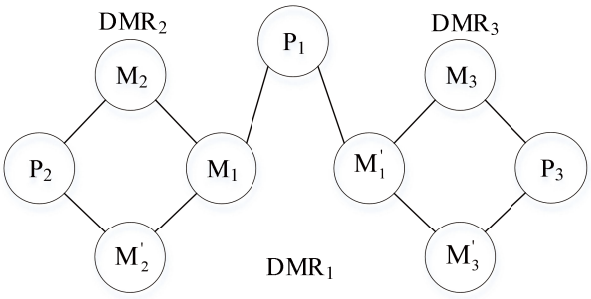

FIGURE 3. Coupling of the duplexer.

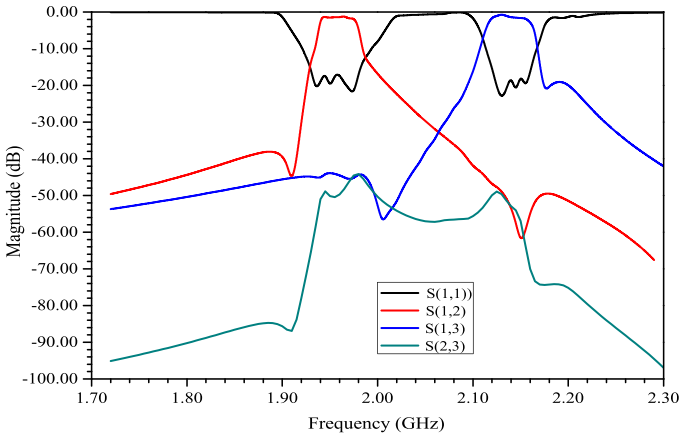

FIGURE 4. Simulated and measured results.

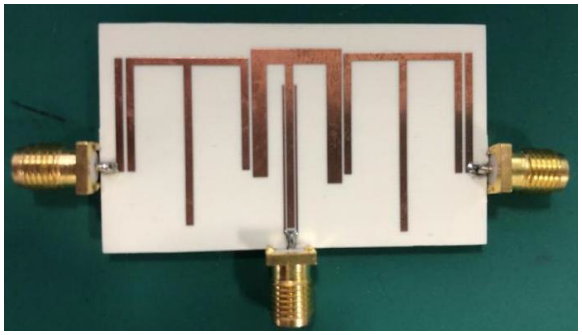

FIGURE 5. Product of the duplexer designed.

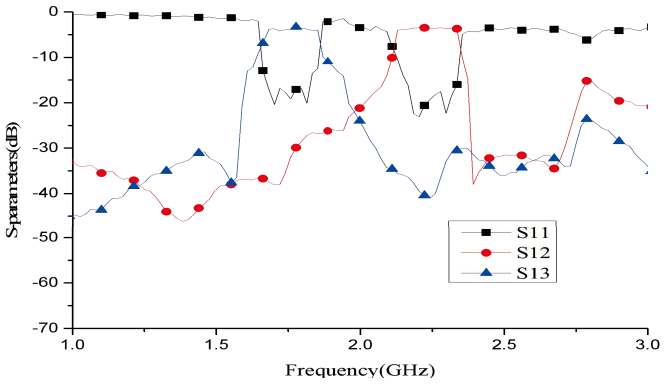

FIGURE 6. The duplexer designed in this paper measures S-parameters.

TABLE 2. Comparation of duplexer parameters from the references.

	Frequencies of the first & second pass band (GHz)	Isolation Level (dB)	Rectangular Coefficient	Circuit Size ($\lambda_g \times \lambda_g$)
[15]	1.95/2.14	$-39/-37$	6.67/6.67	0.38×0.56
[16]	1.5/1.76	$-40/-35$	2.63/2.58	0.34×0.54
[17]	1.95/2.14	$-38/-39$	5.11/6.68	0.43×0.56
[18]	19.1/30	$-34/-34$	4.32/3.67	0.43×0.56
Ours	1.97/2.4	$-44/-48$	2.52/2.28	0.28×0.54

onant frequencies (1.95 GHz and 2.14 GHz), where the two transmission poles are located. A similar way is for DMR_2 and DMR_3. In this way, there are totally three poles on each of the two pass bands.

Not only can the stub-loaded resonators of a duplexer separate the transmitted and received signals, but they also generate an additional transmission pole in each of the frequency bands (1.95 GHz/2.14 GHz) of the duplexer. Signals coming into P_1 (port 1) are divided into two by the public DMR_1 with the two resonant modes M_1 and M_1'. In the odd-mode, the resonant frequency is usually placed at 1.95 GHz on the lower passband and, in the even-mode, 2.14 GHz on the higher passband. Each of the other two E-shaped second-order bandpass resonators on the two sides also has two modes, where M_1 is coupled to the modes of M_2 and M_2' of the left second-order DMR_2, and M_1' to M_3 and M_3' of the right second-order DMR_3.

4. ANALYSIS OF THE MEASURED RESULTS

The design is verified by simulation and product measurements. From the simulation results shown in Figure 4, with $S(1,1) < -10$ dB, two frequency ranges emerge, with the first passband being 1.92 GHz–2 GHz and the second 2.1 GHz–2.18 GHz. Meanwhile, two transmission zeros are introduced in each of the two passbands to enhance the frequency selectivity and isolation levels. The suppression level outside the passbands reaches 40 dB, with the isolation levels of the two central frequencies being -44 dB and -48 dB.

Figure 5 shows the product of the designed E-shaped duplexer, with SMA connectors for the power feed. The duplexer is measured on the E5071C Agilent Network Analyzer. Firstly, the calibration of the analyzer is performed: the open circuit, the short circuit, and the load are connected to port 1 in turn.

Then the starting and ending points of the frequency band to be tested are set. Finally, the two ends of the duplexer are connected to the analyzer. The measured results are shown in Figure 6. It can be found that, when $S(1,1) < 10$ dB, the center frequencies of the two bandwidths are 1.97 GHz and 2.497 GHz; the bandwidths are 1.876 GHz–2.07 GHz and 2.492 GHz–2.558 GHz; and the locations of the transmission zeros are 1.56 GHz and 2.4 GHz. The suppression levels outside the two passbands are both better than -30 dB.

Table 2 compares the performance parameters of the designed duplexer with those in the references. Its isolation levels of -44 dB and -48 dB at the first and second frequency centers are better than those in [15–18]. Besides, its rectangular coefficient (the ratio of the 40 dB bandwidth to the 3 dB bandwidth) is lower than the others, indicating a higher frequency selectivity. Moreover, its circuit size is the smallest among the listed duplexers.

5. CONCLUSION

This letter proposes a novel compact duplexer of three dual-mode E-shaped resonators with strong isolation. The central public resonator and two other dual mode resonators on both sides can produce three transmission poles on each of the lower and higher passbands. Moreover, the three transmission zeros of the microstrip stub-loaded resonators are designed to be above the lower passband, in the middle of the two passbands, and below the upper passband, thus improving the isolation between the two desired channels. Besides, the public resonator can further minimize the size. The principle of the transmission zeros is analyzed in both the odd-mode and even-mode, where the length of the central branch of the E-shaped resonator has influence on the location of the transmission zeros, thus the zeros can be adjusted to meet the requirement.

REFERENCES

[1] Li, J. and W. Yang, "Full duplex high speed data transmission based on partially coupled coils in wireless power transmission systems," *Progress In Electromagnetics Research C*, Vol. 119, 81–96, 2022.

[2] Nguyen, T. and T. Karacolak, "Differential-fed log-periodic dipole array with high isolation for wideband full-duplex communications," *Progress In Electromagnetics Research C*, Vol. 108, 79–87, 2021.

[3] Khani, A. M., M. Fouladian, and J. Mazloum, "Multi layers THz duplexer based on combined graphene patterns," *Solid State Communications*, Vol. 360, 114974, 2023.

[4] Chen, J., L. Li, T. Su, and Y. Chen, "Highly efficient method to calculate S-parameters of microwave filter and duplexer from coupling matrix," *International Journal of RF and Microwave Computer-Aided Engineering*, Vol. 32, No. 3, Mar. 2022.

[5] Li, J., P. Hu, J. Chen, K.-D. Xu, C.-X. Mao, and X. Y. Zhang, "Dual-polarized duplex base-station antenna with a duplexer-integrated balun," *IEEE Antennas and Wireless Propagation Letters*, Vol. 21, No. 2, 317–321, Feb. 2022.

[6] Khani, A. A. M., M. Fouladian, and J. Mazloum, "A wideband tunable microwave graphene-based absorber and duplexer," *Solid State Communications*, Vol. 353, 114797, 2022.

[7] Tao, J. B., Z. J. Tang, Y. L. Zou, *et al.*, "A phase canceling technique to improve SAW duplexer isolation," *Micromachines*, Vol. 14, No. 2, 239, Jan. 2023.

[8] Khani, A. A. M., M. Fouladian, and J. Mazloum, "Two directional THz wave duplexer and filter based on graphene disks and rings," *International Journal of Numerical Modelling: Electronic Networks, Devices and Fields*, Vol. 36, No. 4, e3085, 2023.

[9] Khani, A. A. M., "A graphene-based THz wave duplexer and filter: Switching via gate biasing," *Optik*, Vol. 251, 168432, 2022.

[10] Zhang, X., C. Ma, and D. Cheng, "Compact dual-passband LTCC filter exploiting eighth-mode SIW and SIW hybrid with coplanar waveguide," *Electronics Letters*, Vol. 50, No. 24, 1849–1851, 2014.

[11] Azad, A. R. and A. Mohan, "Sixteenth-mode substrate integrated waveguide bandpass filter loaded with complementary split-ring resonator," *Electronics Letters*, Vol. 53, No. 8, 546–547, 2017.

[12] Chu, P., W. Hong, M. Tuo, K.-L. Zheng, W.-W. Yang, F. Xu, and K. Wu, "Dual-mode substrate integrated waveguide filter with flexible response," *IEEE Transactions on Microwave Theory and Techniques*, Vol. 65, No. 3, 824–830, 2017.

[13] Rezaee, M. and A. R. Attari, "Realisation of new single-layer triple-mode substrate-integrated waveguide and dual-mode half-mode substrate-integrated waveguide filters using a circular shape perturbation," *IET Microwaves, Antennas & Propagation*, Vol. 7, No. 14, 1120–1127, 2013.

[14] Zhu, X.-C., W. Hong, K. Wu, H.-J. Tang, Z.-C. Hao, J.-X. Chen, and P. Chu, "Design and implementation of a triple-mode planar filter," *IEEE Microwave and Wireless Components Letters*, Vol. 23, No. 5, 243–245, 2013.

[15] Chuang, M.-L. and M.-T. Wu, "Microstrip diplexer design using common T-shaped resonator," *IEEE Microwave and Wireless Components Letters*, Vol. 21, No. 11, 583–585, Nov. 2011.

[16] Chen, C.-F., T.-Y. Huang, C.-P. Chou, and R.-B. Wu, "Microstrip diplexers design with common resonator sections for compact size, but high isolation," *IEEE Transactions on Microwave Theory and Techniques*, Vol. 54, No. 5, 1945–1952, May 2006.

[17] Xu, W. Q., M. H. Ho, and C. G. Hsu, "Umts diplexer design using dual-mode stripline ring resonators," *Electronics Letters*, Vol. 43, No. 13, 721–722, Jun. 2007.

[18] Gao, Y., S. Wen, J. Yuan, and X. Xu, "Design of interdigital-filter based diplexer with high isolation and wideband," *High Power Laser and Particle Beams*, Vol. 31, No. 8, 084101, 2019.